membrane and organelle membranes that maintain the integrity of the cell or organelles by creating a semi-impermeable barrier. Phospholipids include phosphatidylcholine (PC), sphingomyelin (SM), phosphatidylserine (PS), and phosphatidylethanolamine (PE) (Fadeel and Xue 2009).

Recently, a profiling strategy based on electrospray tandem mass spectrometry (ESI-MS/MS) has been developed to comprehensively analyze lipid composition in animal and yeast cells (Welti et al. 2002). It requires only simple sample preparation and small samples to identify and quantify lipid species.

Marine red algae emerged as an independent lineage early in the evolution of eukaryotes (Baldauf et al. 2000). The red algal genus *Pyropia* is an important economic marine crop, and *Pyropia haitanensis* is one of the most important species. This species has been cultivated widely along the coasts of South China, especially in Fujian and Zhejiang Provinces (Xie et al. 2009). However, little is known about the profile of membrane lipids of *P. haitanensis* and their changes when induced by elicitors. To reveal the membrane lipid profiles and how lipid species change under stress conditions is important to understand membrane and cell functions. In our previous research, agaro-oligosaccharides induced the oxidative burst and the release of volatile organic compounds in *P. haitanensis* (Wang et al. 2013).

In this study we use ultra-performance liquid chromatography-electrospray ionization-quadrupole-time of flight mass spectrometry (UPLC-ESI-Q-TOF-MS) to qualitatively and quantitatively determine the lipids in *P. haitanensis* and their changes in response to treatment with agaro-oligosaccharides.

Materials and methods

Acetonitrile, isopropanol, formic acid, and sodium formate (liquid chromatography-mass spectrometry (LC-MS) grade) were from Sigma-Aldrich (USA). Distilled water was filtered through a Milli-Q system (Millipore, USA). Leucine-enkephalin was from Sigma-Aldrich. Standards (phosphatidylcholine (18:1/14:0), phosphatidylglycerol (16:0/18:1), and phosphatidylethanolamine (18:1/18:1)) were obtained from the Avanti Polar Lipids, Inc. (USA). Glycolipids standards including monogalactosyldiacylglycerol, digalactosyldiacylglycerol, and sulfoquinovosyldiacylglycerol were from Lipid Products (UK).

Plant material and cultivation treatments

The marine red alga *P. haitanensis* was obtained from the coast of Xiangshan, Zhejiang Province, China. Young fronds (2–10 cm in length) were collected and transported to the laboratory. They were kept in flasks (20–30 mg fresh weight of algae per flask) containing 30 L of 0.45-μm filtered seawater at 18±1 °C, under constant aeration and photon flux density of 45 to 54 μmol photons m^{-2} s^{-1} with a photoperiod of 12-h light/12-h dark for 2 days. Just before the start of the experiment, five individuals were harvested as control material. Agaro-oligosaccharides (100 μg mL^{-1}) were added in the culture medium to elicit defense responses in *P. haitanensis*. Algal samples were harvested after 1 and 3 h of treatment with agaro-oligosaccharides. No nutrients were added during the experiment. All experiments were performed in five replicates and reported as average±one standard deviation. At the end of the experiment, the algae were frozen in liquid nitrogen and stored at −80 °C for analysis.

Lipid analysis

Samples were extracted according to Bligh and Dyer (1959). The sample was dried under nitrogen gas and dissolved in 0.5-mL methanol for UPLC-qTOF-MS analysis.

Chromatographic separation was performed on an ACQUI-TY UPLC BEH C8 analytical column (100× 2.1 mm, 1.7 μm, Waters, USA) using an ACQUITY UPLC system (Waters). Optimal separation was achieved with a gradient elution using (A) water (containing 0.1 %*v/v* formic acid and 0.001 %*v/v* sodium formate) and (B) a mixture of methanol/acetonitrile/isopropanol (1:2:1, *v/v/v*, containing 0.1 %*v/v* formic acid and 0.001 %*v/v* sodium formate) at a flow rate of 0.35 mL min^{-1}. The gradient (time, %B) was set as (0, 5), (5, 50), (30, 100), (35, 100), and (36, 5). The injection volume was 5 μL. An aliquot of each sample was injected into the column, and 25 % of the effluent was split into the mass spectrometer.

Mass spectrometry was performed on a Q-TOF Premier (Waters) operating in both negative ion and positive ion electrospray ionization (ESI) modes. The ESI conditions were capillary voltage 3.0 kV (positive modes) and 2.6 kV (negative modes), sampling cone voltage 30–60 V, source temperature 120 °C, desolvation temperature 250 °C, nebulization gas flow 400 L h^{-1}, and cone gas flow 50 L h^{-1}. The collision energy for tandem mass spectrometry (MS) was scanned from 15 to 55 eV. The MS acquisition rate was 0.3 s with a 0.02-s inter-scan delay. Data were collected in the centroid mode from 80 to 1,200*m/z* in MS scanning. All analyses were performed using the lock spray to ensure accuracy and reproducibility. Leucine-enkephalin was used as the lock mass at a concentration of 200 ng mL^{-1} and a flow rate of 10 μL min^{-1}, generating an $[M+H]^+$ ion of 556.2771 Da in ESI^+ mode, and an $[M-H]^-$ ion of 554.2615 Da in ESI^- mode. The lock spray frequency was set at 10 s.

Data analysis

The UPLC/MS data preprocessing was performed with MarkerLynx 4.1 software (Waters, USA). For each sampling

time, differences between the treatments and control were analyzed via one-way analyses of variance (ANOVA) followed by a post hoc multiple comparisons test (Dunnett's test). The content of lipid in *P. haitanensis* was assessed by ANOVA.

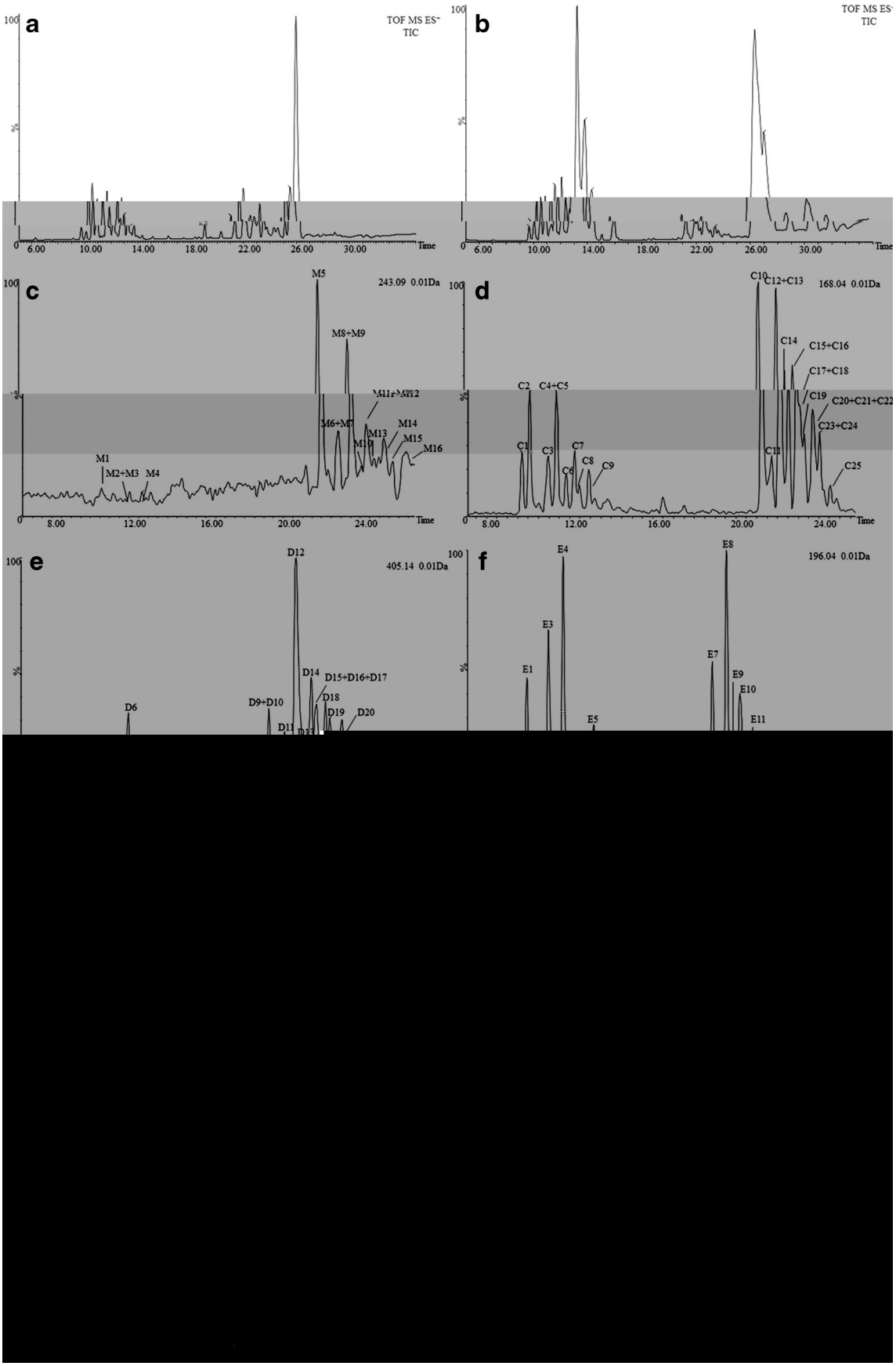
a
TOF MS ES+
TIC
b
TOF MS ES+
TIC
c
243.09 0.01Da
M1
M2+M3
M4
M5
M6+M7
M8+M9
M10
M11+M12
M13
M14
M15
M16
d
168.04 0.01Da
C1
C2
C3
C4+C5
C6
C7
C8
C9
C10
C12+C13
C14
C15+C16
C17+C18
C19
C20+C21+C22
C23+C24
C25
e
405.14 0.01Da
D6
D9+D10
D11
D12
D14
D15+D16+D17
D18
D19
D20
f
196.04 0.01Da
E1
E3
E4
E5
E7
E8
E9
E10
E11
Time

◀ **Fig. 1** Total ion chromatogram of the lipid mixture extracted from *Pyropia haitanensis* at a low collision energy of 5 V in the positive mode with the MS^E technique **(a)**; total ion chromatogram of the lipid mixture extracted from *Pyropia haitanensis* at a low collision energy of 5 V in the negative mode with the MS^E technique **(b)**; extracted ion chromatogram of *m/z* 243.08 for characteristic product ion of MGDG in *Pyropia haitanensis* from the high collision energy scans (ramp of 15–55 V) in the positive mode with the MS^E technique **(c)**; extracted ion chromatograms of *m/z* 168.04 for characteristic product ion of PC in *Pyropia haitanensis* from the high collision energy scans (ramp of 15–55 V) in the negative mode with the MS^E technique **(d)**; extracted ion chromatogram of *m/z* 405.14 for characteristic product ion of DGDG in *Pyropia haitanensis* from the high collision energy scans (ramp of 15–55 V) in the positive mode with the MS^E technique **(e)**; extracted ion chromatograms of *m/z* 196.04 for characteristic product ion of PE in *Pyropia haitanensis* from the high collision energy scans (ramp of 15–55 V) in the negative mode with the MS^E technique **(f)**; extracted ion chromatograms of *m/z* 225.01 for characteristic product ion of SQDG in *Pyropia haitanensis* from the high collision energy scans (ramp of 15–55 V) in the negative mode with the MS^E technique *(g)*; extracted ion chromatograms of *m/z* 153.00 for characteristic product ion of PA in *Pyropia haitanensis* from the high collision energy scans (ramp of 15–55 V) in the negative mode with the MS^E technique **(h)**; extracted ion chromatogram of *m/z* 171.01 for characteristic product ion of PG in *Pyropia haitanensis* from the high collision energy scans (ramp of 15–55 V) in the negative mode with the MS^E technique **(i)**. A1: PA (20:5/20:5), A2: PA (20:5/20:4), A3: unknown, A4: PA (20:4/20:4), A5: unknown, A6: unknown, A7: unknown, A8: unknown; C1: unknown, C2: LysoPC (20:5), C3: unknown, C4: LysoPC (18:2), C5: LysoPC (20:4), C6: unknown, C7: LysoPC (20:3), C8: LysoPC (18:3), C9: LysoPC (18:1), C10: PC (20:5/20:5), C11: unknown, C12: PC (20:5/20:4), C13: PC (18:2/20:5), C14: PC (20:5/20:3), C15: PC (16:0/20:5), C16: PC (20:4/20:4), C17: PC (20:5/18:1), C18: PC (18:3/20:5), C19: PC (20:4/20:3), C20: PC (16:0/20:4), C21: PC (16:0/18:2), C22: PC (20:4/18:1), C23: PC (20:3/20:3), C24: PC (16:0/20:3), C25: PC (16:0/18:1); D1: LysoDGDG (20:5), D2: LysoDGDG (18:2), D3: LysoDGDG (16:0), D4: LysoDGDG (18:1), D5: unknown, D6: unknown, D7: unknown, D8: unknown, D9: DGDG (16:0/16:0), D10: DGDG (20:5/20:5), D11: DGDG (20:5/18:2), D12: DGDG (20:5/16:0), D13: DGDG (20:4/16:0), D14: DGDG (16:0/18:2), D15: DGDG (18:1/18:2), D16: DGDG (20:2/18:2), D17: DGDG (16:0/20:3), D18: DGDG (16:0/18:1), D19: DGDG (20:2/18:1), D20: unknown, D21: unknown, D22: DGDG (18:0/18:2); E1: LysoPE (20:5), E2: unknown, E3: LysoPE (20:4), E4: unknown, E5: unknown, E6: unknown, E7: PE (20:5/20:5), E8: PE (20:5/20:4), E9: PE (20:4/20:4), E10: unknown, E11: unknown, E12: unknown, E13: unknown; G1: unknown, G2: LysoPG (16:1), G3: LysoPG (16:0), G4: unknown, G5: PG (20:5/16:1), G6: PG (20:5/16:0), G7: unknown, G8: PG (20:4/16:0), G9: unknown, G10: PG (20:2/16:0), G11: PG (20:1/16:0), M1: LysoMGDG (20:5), M2: LysoMGDG (18:2), M3: LysoMGDG (20:4), M4: LysoMGDG (16:0), M5: MGDG (20:5/20:5), M6: MGDG (20:4/20:5), M7: MGDG (20:5/18:2), M8: MGDG (20:5/16:0), M9: MGDG (20:4/18:2), M10: MGDG (20:4/18:1), M11: MGDG (20:4/16:0), M12: MGDG (16:0/18:2), M13: MGDG (16:0/20:3), M14: MGDG (16:0/18:1), M15: unknown, M16: unknown, S1: LysoSQDG (16:0), S2: unknown, S3: SQDG (20:5/16:0), S4: unknown, S5: SQDG (20:4/16:0), S6: SQDG (18:2/16:0), S7: SQDG (16:0/16:0), S8: SQDG (18:0/16:0)

agaro-oligosaccharide treatment, massive declines in the levels of PC such as PC (18:3/20:5) and PE such as PE (20:5/20:4) occurred, but PA such as PA (20:4/20:4), lysoPC such as LysoPC (20:5), and lysoPE such as LysoPE (20:5) increased dramatically (Tables 1 and 2). These changes suggested a rise in lipolytic activities after treatment with agaro-oligosaccharides. The loss occurred in almost all species of PC and PE, with most decreases in PE (20:5/20:4) and PC (18:3/20:5). The PG, MGDG, SQDG, and DGDG levels, such as PG (20:5/16:1), SQDG (20:5/16:0), MGDG (20:5/20:5), and DGDG (20:5/20:5), tended to decline, 3 h after agaro-oligosaccharide treatment, comparing with 1 h after agaro-oligosaccharide treatment. The galactolipids such as MGDGs did not change much, 3 h after agaro-oligosaccharide treatment, comparing with 1 h agaro-oligosaccharide treatment. The large decline in the major types of membrane phospholipids (such as PC (18:3/20:5), PE (20:5/20:5)) but not galactolipids (such as MGDGs) after 3 h of treatment with agaro-oligosaccharides suggested that phospholipases were activated to a greater extent than galactolipases. The increase in PA and lysophospholipid levels indicated that the hydrolytic activity was increased by exposure to agaro-oligosaccharides.

Discussion

We used the ESI-MS/MS method for rapid analysis of the composition of membrane lipids that include glycolipids in photosynthetic membrane and plasma membrane. The easy sample preparation and relatively short analysis time permit the quick profiling of membrane lipids in *P. haitanensis* and their changes triggered by agaro-oligosaccharides. Our results indicated that the content of acidic lipids (SQDG) in *P. haitanensis* was significantly higher than in higher plants and strongly resembles the lipid composition of cyanobacteria. In higher plants, lipids are usually synthesized by two distinct pathways, the prokaryotic and eukaryotic pathways. The synthesized lipids by the prokaryotic pathway have exclusively C16 fatty acids at the *sn*-2 position of glycerol, while the lipids synthesized by the eukaryotic pathway have C18 fatty acids (Xu et al. 2002). The positional distribution of fatty acids of the individual lipid class of *P. haitanensis* indicated that MGDG and DGDG have a typical mixed biosynthetic pathway including both prokaryotic pathway and eukaryotic pathway, because the fatty acids at *sn*-2 position include both C16 and C18 fatty acids. SQDG and PG are biosynthesized through the prokaryotic pathway exclusively within the chloroplast because the fatty acids at *sn*-2 position are C16 fatty acids in SQDG and PG. We found that the *sn*-2 position of the glycerol backbone in MGDG and DGDG was also occupied by C20 fatty acids, *sn*-2 position of PC was occupied by C18 fatty acids or C20 fatty acids, and *sn*-2 position of PE and PA was occupied by C20 fatty acids in *P. haitanensis*. These findings provide clues on the evolutionary process of plant. During the evolution of eukaryotes to higher plant, the 20 carbon metabolism may be discarded, and only the C18 fatty acid metabolism is retained. The results reported here suggest that red algal *P. haitanensis* is an ancient plant species.

Table 1 Content of photosynthetic glycerolipids in *Pyropia haitanensis*. The same superscripted letter indicates no significant difference (Dunnett's test, $P<0.05$) after treatment with agaro-oligosaccharides

Identification	Content (nmol g^{-1})	Treated group (1 h, nmol g^{-1})	Treated group (3 h, nmol g^{-1})
PG (20:2/16:0)	9.96±1.86^{a}	18.82±1.05^{b}	17.02±0.94^{b}
PG (20:4/16:0)	16.86±1.26^{a}	32.44±2.35^{b}	32.60±2.26^{b}
PG (20:1/16:0)	105.76±5.89^{a}	138.43±11.56^{b}	145.68±13.65^{b}
PG (20:5/16:1)	152.51±8.04	169.43±11.39	162.12±7.79
PG (20:5/16:0)	210.54±13.10^{a}	271.97±37.33^{b}	296.70±17.60^{b}
Lyso-PG (16:1)	72.77±6.55^{a}	44.75±8.70^{b}	56.80±9.90^{ab}
Lyso-PG (16:0)	99.06±11.24^{a}	86.87±8.27^{a}	128.02±10.00^{b}
SQDG (18:0/16:0)	33.86±1.89	36.80±2.13	34.49±0.72
SQDG (18:2/16:0)	26.65±2.36^{a}	39.60±3.48^{b}	42.43±2.47^{b}
SQDG (20:4/16:0)	152.65±11.88^{a}	264.28±13.96^{b}	252.39±14.30^{b}
SQDG (16:0/16:0)	361.13±15.82^{a}	501.28±33.01^{b}	521.11±49.78^{b}
SQDG (20:5/16:0)	1318.22±227.16^{ab}	1529.17±72.31^{a}	1213.39±22.93^{b}
Lyso-SQDG (16:0)	651.28±54.40^{a}	496.51±34.27^{b}	699.43±30.25^{a}
MGDG (20:4/18:1)	9.91±1.51^{a}	15.31±0.28^{b}	15.06±2.34^{b}
MGDG (16:0/20:3)	16.93±3.26^{a}	23.25±2.06^{ab}	26.05±4.82^{b}
MGDG (20:4/20:5)	25.67±1.72^{a}	37.86±3.79^{b}	31.41±2.71^{a}
MGDG (20:5/18:2)	24.95±3.78^{a}	28.74±3.99^{ab}	32.63±2.99^{b}
MGDG (20:4/18:2)	16.66±1.70^{a}	31.97±3.17^{b}	33.42±4.25^{b}
MGDG (16:0/18:2)	36.69±2.64^{a}	45.91±0.48^{b}	47.46±3.53^{b}
MGDG (16:0/18:1)	43.62±3.27^{a}	49.32±3.61^{ab}	55.14±5.29^{b}
MGDG (20:4/16:0)	65.01±11.24^{a}	114.96±11.80^{b}	107.87±5.12^{b}
MGDG (20:5/16:0)	231.32±23.69^{a}	273.95±8.08^{b}	275.49±16.05^{b}
MGDG (20:5/20:5)	328.54±20.96^{a}	404.97±29.90^{b}	384.84±26.92^{b}
Lyso-MGDG (20:4)	49.51±4.52^{a}	58.63±4.61^{b}	64.41±4.34^{b}
Lyso-MGDG (18:2)	53.15±3.78^{a}	49.13±6.86^{a}	73.08±4.33^{b}
Lyso-MGDG (16:0)	211.91±19.01^{a}	239.53±15.33^{ab}	267.67±12.39^{b}
Lyso-MGDG (20:5)	287.09±33.48^{a}	317.06±26.67^{ab}	342.63±15.79^{b}
DGDG (16:0/16:0)	0.49±0.16^{a}	2.77±0.47^{b}	0.94±0.23^{a}
DGDG (16:0/20:3)	3.36±0.25	3.50±0.16	3.54±0.33
DGDG (18:1/18:2)	3.46±0.38	4.09±0.29	4.12±0.41
DGDG (20:2/18:2)	3.67±0.38	4.13±0.34	4.16±0.39
DGDG (20:5/18:2)	4.43±0.48	4.83±0.25	4.93±0.24
DGDG (20:2/18:1)	4.97±0.37	5.76±0.26	5.97±0.88
DGDG (20:4/16:0)	6.40±0.70^{a}	8.18±0.04^{b}	8.09±0.48^{b}
DGDG (18:0/18:2)	7.07±0.74 ^{a}	8.31±1.61 ^{a}	12.93±1.33^{b}
DGDG (16:0/18:1)	10.62±1.00^{a}	13.89±0.93^{b}	13.76±1.29^{b}
DGDG (16:0/18:2)	12.90±0.57^{a}	15.32±0.55^{b}	14.67±0.34^{b}
DGDG (20:5/20:5)	11.34±0.82^{a}	15.52±2.00^{b}	15.07±1.26^{b}
DGDG (20:5/16:0)	25.25±0.44^{a}	32.30±4.02^{b}	30.02±3.14^{ab}
Lyso-DGDG (20:5)	2.20±0.21	2.19±0.21	2.66±0.40
Lyso-DGDG (18:1)	9.43±0.79	8.30±0.26	9.59±1.18
Lyso-DGDG (18:2)	9.56±1.53	9.82±0.75	10.62±1.30
Lyso-DGDG (16:0)	67.34±6.61^{a}	73.66±4.68^{ab}	82.73±6.72^{b}

Significant changes in membrane lipid species occurred when *P. haitanensis* were treated with agaro-oligosaccharides. The results demonstrated that *P. haitanensis* had developed mechanisms to alter lipid compositions to cope with elicitor through lipid synthesis and degradation. At first, agaro-oligosaccharides induced an increase in total membrane lipids including the galactolipids and phospholipids, while the levels of lyso-galactolipids and lyso-phospholipids decreased. These

results also suggested that agaro-oligosaccharides induced changes of lipids in both chloroplasts and plasma membranes. But with the increased time of treatment, a large decline was observed in major types of membrane phospholipids but not galactolipids, suggesting that the lipid change occurred mainly at the plasma membrane and phospholipases were activated to a greater extent than galactolipases.

Signal-induced production of PA in the cell is accomplished by two principal routes: phospholipase D (PLD)-mediated hydrolysis of membrane lipids and DAG-kinase-mediated phosphorylation of DAG (Wang 2004). Laxalt and Munnik (2002) reported that phosphatidic acid (PA) was a second messenger in plant defense signaling pathways. In addition, PA serves as a substrate and/or an activator for enzymes that promote the formation of other lipid regulators, such as lysoPA, free fatty acids, diacylglycerol (DAG), DAG-pyrophosphate, and oxylipins (Wang 2005).

Zhang et al. (2003) reported that PA is involved in the alleviation of H_2O_2

Acknowledgments This work was supported by the Scientific Research Fund of the Zhejiang Provincial Education Department Y201121083, the Zhejiang Marine Biotechnology Innovation Team (2010R50029), and the Ningbo Marine Algae Biotechnology Team (2011B81007).

References

Baldauf SL, Roger AJ, Wenk-Siefert I, Doolittle WF (2000) A kingdom-level phylogeny of eukaryotes based on combined protein data. Science 290:972–977

Benning C (1998) Membrane lipids in anoxygenic photosynthetic bacteria. In: Siegenthaler PA, Murata N (eds) Lipids in photosynthesis: structure, function and genetics, vol 6, advances in photosynthesis and respiration. Springer, Dordrecht, pp 41–46

Bligh EG, Dyer WJ (1959) A rapid method for total lipid extraction and purification. Can J Biochem Physiol 37:911–917

Fadeel B, Xue D (2009) The ins and outs of phospholipid asymmetry in the plasma membrane: roles in health and disease. Crit Rev Biochem Mol Biol 44:264–277

Han XL, Gross RW (1995) Structural determination of picomole amounts of phospholipids via electrospray ionization tandem mass spectrometry. J Am Soc Mass Spectrom 6:1202–1210

Hvattum E, Hagelin G, Larsen A (1998) Study of mechanisms involved in the collision-induced dissociation of carboxylate anions from glycerophospholipids using negative ion electrospray tandem quadrupole mass spectrometry. Rapid Commun Mass Spectrom 12: 1405–1409

Laxalt AM, Munnik T (2002) Phospholipid signalling in plant defence. Curr Opin Plant Biol 5:332–338

Lu N, Wei D, Chen F, Yang ST (2012) Lipidomic profiling and discovery of lipid biomarkers in snow alga *Chlamydomonas nivalis* under salt stress. Eur J Lipid Sci Tech 114:253–265

Sommer U, Herscovitz H, Welty FK, Costello CE (2006) LC-MS based method for the qualitative and quantitative analysis of complex lipid mixtures. J Lipid Res 47:804–814

Uemura M, Steponkus PL (1997) Effect of cold acclimation on the lipid composition of the inner and outer membrane of the chloroplast envelope isolated from rye leaves. Plant Physiol 114:1493–1500

Wang SY, Lin HS (2006) Effect of plant growth temperature on membrane lipids in strawberry (*Fragaria× ananassa* Duch.). Sci Horticult 108:35–42

Wang XJ, Chen HM, Chen JJ, Luo QJ, Xu JL, Yan XJ (2013) Response of *Pyropia haitanensis* to agaro-oligosaccharides evidenced mainly by activation of the eicosanoid pathway. J Appl Phycol 25:1895–1902

Wang XM (2004) Lipid signaling. Curr Opin Plant Biol 7:329–336

Wang XM, Li WQ, Li MY, Welti R (2006) Profiling lipid changes in plant response to low temperatures. Physiol Plant 126:90–96

Wang XM (2005) Regulatory functions of phospholipase D and phosphatidic acid in plant growth, development, and stress responses. Plant Physiol 139:566–573

Welti R, Li W, Li M, SangY BH, Zhou HE, Rajashekar CB, Williams TD, Wang X (2002) Profiling membrane lipids in plant stress responses. Role of phospholipase Dα in freezing-induced lipid changes in Arabidopsis. J Biol Chem 277:31994–32002

Xie CT, Chen CS, Ji DH, Xu Y (2009) Characterization, development and exploitation of EST-derived microsatellites in *Porphyra haitanensis* Chang et Zheng (Bangiales, Rhodophyta). J Appl Phycol 21:367–374

Xu JL, Chen DY, Yan XJ, Chen JJ, Zhou CX (2010) Global characterization of the photosynthetic glycerolipids from a marine diatom *Stephanodiscus* sp. by ultra performance liquid chromatography coupled with electrospray ionization-quadrupole-time of flight mass spectrometry. Anal Chim Acta 663:60–68

Xu YN, Wang ZN, Yan XJ, Lin W, Li LB, Kuang TY (2002) Positional distribution of fatty acids on the glycerol backbone during the biosynthesis of glycerolipids in *Ectocarpus fasciculatus*. Chin Sci Bull 47:1802–1806

Yan XJ, Li HY, Xu JL, Zhou CX (2010) Analysis of phospholipids in microalga *Nitzschia closterium* by UPLC-Q-TOF-MS. Chin J Oceanol Limnol 28:106–112

Zhang WH, Wang CX, Qin CB, Wood T, Olafsdottir G, Welti R, Wang XM (2003) The oleate-stimulated phospholipase D, PLDδ, and phosphatidic acid decrease H_2O_2-induced cell death in *Arabidopsis*. Plant Cell 15:2285–2295